ExtrudeNet: Unsupervised Inverse Sketch and Extrude for Shape Parsing – Supplementary Materials –

A Propositions and Proofs

Proposition 1. *The area bounded by the curve generated by rBézierSketch is a star-shaped set.*

Proof: Consider an arbitrary ray cast from the origin. Since the polygon generated by connecting all the control points in order is homeomorphic to the origin-centered unit circle, the ray will intersect the polygon at least once. On the other hand, based on the construction of the control points of the rational Bézier curve, when we travel along the polygon in the counter-clock direction, the polar angle is monotonically increasing, which means that the ray will not intersect the polygon more than once. Therefore the ray intersects the Bézier control polygon only once, so does it intersect the profile curve, which is confirmed by the continuity of the curve and the variation diminishing property of rational Bézier curves. The variation diminishing property says that for an arbitrary line, the number of intersections with the curve will not be greater than the number of intersections with the control polygon [1]. Hence any point on the profile curve can be visible to the origin. ■

Proposition 2. *Let the polar angles be given by Eq.2. If* $\rho_0^k = \rho_3^k$, $\rho_1^k = \rho_2^k = \frac{\rho_0^k}{\cos(\theta)}$, *and* $w_1^k = w_2^k = \frac{1}{3}\left(1 + 2\cos\left(\frac{\pi}{N}\right)\right)$, *then the rational Bézier curve of (1) defines a circular arc, as shown in Fig.3 (left).*

Proof: Consider triangle $\triangle O P_0^k P_1^k$ shown in Fig.3 (left). If $\rho_1^k = \frac{\rho_0^k}{\cos(\theta)}$, $\angle O P_0^k P_1^k$ is a right angle. Then $\|P_0^k P_1^k\| = \rho_0^k \tan(\theta)$. Since $\theta = \frac{\pi}{2N} + \tan^{-1}\left(\frac{1}{3}\tan\left(\frac{\pi}{2N}\right)\right)$, we thus have

$$
\begin{aligned}
\|P_0^k P_1^k\| &= \rho_0^k \frac{\tan\left(\frac{\pi}{2N}\right) + \frac{1}{3}\tan\left(\frac{\pi}{2N}\right)}{1 - \tan\left(\frac{\pi}{2N}\right) \cdot \frac{1}{3}\tan\left(\frac{\pi}{2N}\right)} \\
&= \rho_0^k \frac{\frac{4}{3}\frac{\sin\left(\frac{\pi}{2N}\right)}{\cos\left(\frac{\pi}{2N}\right)}}{1 - \frac{1}{3}\left(\sec^2\left(\frac{\pi}{2N}\right) - 1\right)} \\
&= \rho_0^k \frac{4\sin\left(\frac{\pi}{2N}\right)\cos\left(\frac{\pi}{2N}\right)}{4\cos^2\left(\frac{\pi}{2N}\right) - 1} \\
&= \rho_0^k \frac{2\sin\left(\frac{\pi}{N}\right)}{1 + 2\cos\left(\frac{\pi}{N}\right)}.
\end{aligned}
$$

Similar analysis applies to the other end of the Bézier curve. It can be easily verified that these equations together with the chosen weights in the proposition

make the conditions given in [2] be satisfied, which ensure that the generated rational cubic Bézier curve is an circular arc, and thus we arrive at the conclusion. ■

Proposition 3. *If the control points and weights satisfy*

$$P_0^{k+1} = P_3^k = \frac{\rho_2^k P_1^{k+1} + \rho_1^{k+1} P_2^k}{\rho_2^k + \rho_1^{k+1}}, \ \frac{w_2^k}{w_1^{k+1}} = \frac{\rho_1^{k+1}}{\rho_2^k}, \tag{S.1}$$

curve segments $C_{k+1}(t)$ and $C_k(t)$ meet at P_0^{k+1} with C^1 continuity.

Proof: Consider curve segments $C_k(t)$ and $C_{k+1}(t)$. First, $P_0^{k+1} = P_3^k$ assures C^0 continuity of the two segments. Second, from Eq.S.1, we have

$$\rho_2^k (P_1^{k+1} - P_0^{k+1}) = \rho_1^{k+1} (P_3^k - P_2^k) \tag{S.2}$$

or

$$w_1^{k+1} (P_1^{k+1} - P_0^{k+1}) = w_2^k (P_3^k - P_2^k). \tag{S.3}$$

Eq.S.2 implied that P_0^{k+1} or P_3^k does lie on the bisector of angle $\angle P_2^k O P_1^{k+1}$. Eq.S.3 means $C_k'(1) = C_{k+1}'(0)$. This is because

$$C_k'(1) = 3\left((P_3^k - w_2^k P_2^k) - (1 - w_2^k) P_3^k\right) = 3 w_2^k (P_3^k - P_2^k)$$

and similarly,

$$C_{k+1}'(0) = 3 w_1^{k+1} (P_1^{k+1} - P_0^{k+1}).$$

Therefore $C_{k+1}(t)$ and $C_k(t)$ meet at P_0^{k+1} with C^1 continuity. ■

B More Ablation Studies

Ablation on Number of Sample Points Per Curve As discussed in Fig.10, sample rate plays an important role on the accuracy of the approximation. To further demonstrate that Sketch2SDF can work with a relative small sampling rate, we vary the sampling rate and train ExtrudeNet separately, as shown in the Tab.A, even with a small sample rate (80 per sketch) ExtrudeNet still manages to generate comparable results.

Table A. Chamfer Distances of Airplane class under different sample rate. We can see that ExtrudeNet performs comparably even under small number of sample points.

Sample Rate	400	320	160	80
CD	**0.664**	0.702	0.726	0.725

Fig. A. Reconstruction results by setting constraints on the extrusion plane orientation. **Left**: Top Extrude. **Middle**: Side Extrude. **Left**: Front Extrude.

Ablation on Number of Bezier Curve Per Sketch rBézierSketch can be configured to generate sketches with different number of Bezier Curves. Highly flexible sketch can be achieved via using a large number of curves, however, this increase the computation cost and also gives network too much degree of freedom, making the network much harder to train.

Table B. Performance of ExtrudeNet under different numbers of Curves. We can see that too few Bézier curves is not flexible enough while large number of curve makes network harder to train.

# Curves	2	4	6	8
CD	0.754	**0.664**	0.722	1.09

Ablation on Sketch Plane Orientation Three-view-drawing is a popular drawing method that placing the sketch plane on 3D coordinate planes. In this ablation, we study the effect of the ExtrudeNet's performance under constraint sketch plane orientation, see Tab.C. Interestingly, the results are consistent with how human tends to draw shapes (from top and front).

Table C. We train ExtrudeNet with constraint sketch plane orientation, we can see that freely placed sketch plane yields the best result.

Orientation	side	top	front	free
CD	3.291	0.821	0.733	**0.664**

Effect of Padding. As Bézier Sketches are very flexible and locally supported, only the control points that have testing points in their proximity are updated. Note that we add 15% padding on each side of the mesh bounding box. Without padding, artifacts that "over-shoot" outside the bounding box can be generated (Fig.B). Adding padding when sampling the testing points can solve this problem, as "over-shot" shapes in the padded region will incur a higher loss which forces all the control points to be updated.

C More Visualizations

We have created a video for better visualization, see attached. The video is composed of two sections. First section illustrates ExtrudeNet in detail with special attention on the "Sketch" and "Extrude" process. Note that, to better visualize individual extruded shapes, we using UNION as the assembly method, thus the final reconstruction results are worse than the complete ExtrudeNet. Second section of the video shows detailed reconstructed results. We have also attached more rendered results in Fig.C.

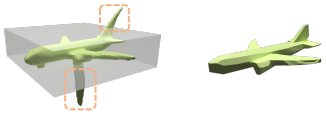

Fig. B. Left: Without padding the generated mesh contains artifacts that overshoot the gray bounding box. Right: Result with padding.

Fig. C. More visualization of ExtrudeNet results

References

1. Farin, G.: Curves and Surfaces for CAGD: A Practical Guide. Morgan Kaufmann Publishers Inc., San Francisco, CA, USA, 5th edn. (2001) 1
2. Wang, G.J.: Rational cubic circular arcs and their application in cad. Computers in Industry **16**(3), 283–288 (1991). https://doi.org/https://doi.org/10.1016/0166-3615(91)90066-I, https://www.sciencedirect.com/science/article/pii/0166361591900066I 2